Desalination and Water Treatment
www.deswater.com

doi: 10.1080/19443994.2016.1187090

57 (2016) 28349–28362
December

Taylor & Francis
Taylor & Francis Group

Mechanistic and spectroscopic investigations of Ru^{3+}-catalyzed oxidative degradation of azidothymidine by heptavalent manganese at environmentally relevant pH

Raviraj M. Kulkarni[a,*], Vijaykumar S. Bhamare[a], B. Santhakumari[b]

[a]*Department of Chemistry, KLS Gogte Institute of Technology (Autonomous), Visvesvaraya Technological University, Belagavi 590 008, Karnataka, India, Tel. +91 8312498511; Fax: +91 8312441909; emails: ravirajmk@git.edu (R.M. Kulkarni), vbhamare37@gmail.com (V.S. Bhamare)*

[b]*Center for Materials Characterization Division, CSIR-National Chemical Laboratory, Pune 411008, Maharashtra, India, Tel. +91 2025902296; email: b.santhakumari@ncl.res.in*

Received 19 February 2016; Accepted 26 April 2016

ABSTRACT

The rapid increase in the population across the world has increased the consumption of pharmaceutical substances. These pharmaceutical substances have penetrated into the water through various ways. Mechanistic and spectroscopic investigations of Ru^{3+}-catalyzed oxidative degradation of azidothymidine (AZT) by heptavalent manganese was studied for the first time. The values of pH-dependent apparent second-order rate constant show that Ru^{3+} accelerates the rate of the oxidative degradation of AZT by heptavalent manganese eight times faster than uncatalyzed reaction. Ru^{3+} catalytic oxidative degradation of AZT by heptavalent manganese was greatly depending on the pH. The removal of the AZT by heptavalent manganese in the presence of Ru^{3+} shows unit order with respect to heptavalent manganese, Ru^{3+}, and AZT. The influences of dielectric constant, ionic strength, pH, addition of monomer, variation in catalyst concentration, etc. on the rate of the reaction were studied thoroughly and discussed in detail. The eight different products produced during the reaction were analyzed using the high-resolution mass spectrometry. Activation parameters were determined from variation in temperature during the reaction. The catalytic plausible mechanism was projected in which Ru^{3+} is oxidized to higher oxidation states of ruthenium by heptavalent manganese at environmentally relevant pH.

Keywords: Catalysis; Degradation; Azidothymidine; Heptavalent manganese; Kinetics; Mechanism

1. Introduction

The World Health Organization (WHO) 2009 report concludes that there is a need of the systematic investigation for the better understanding of the transport, occurrence, and fate of pharmaceutical compounds (PhACs) in drinking water [1]. These PhACs penetrate into the drinking water through many ways. It is predicted that these PhACs are not disposed correctly and mixed into drinking water [2]. Many reviews have been published on the presence of pharmaceutical residues in the potable water [3,4].

---

*Corresponding author.

The ubiquitous use of PhACs has resulted in the contamination of water. These PhACs present in water have adverse effects on human beings and the environment [5–7]. In order to reduce these contaminants present in the water, various oxidation techniques have been proposed [8,9].

The antiretroviral drug azidothymidine (AZT) or zidovudine (ZDV) is used for treating human Immunodeficiency virus/acquired immunodeficiency syndrome infection. AZT is a nucleoside analog reverse transcriptase inhibitor (NTRI). AZT is a white to light brown color crystalline solid. The molecular formula and molecular weight of AZT are $C_{10}H_{13}N_5O_4$ and 267.24 g/mol, respectively [10,11]. The pK_a value (dissociation constant) for antiretroviral drug AZT is 9.68 [12]. The antiretroviral drug AZT is soluble in water and its solubility is 25 mg mL^{-1} at 25℃ [13]. The chemical name of the AZT is 3´-Azido-3´-deoxythymidine. The structure of AZT is shown in Fig. 1.

Heptavalent manganese has been extensively used for the treatment of drinking water to remove contaminants present in the water [14,15]. Heptavalent manganese is found to be better and efficient oxidizing agent as compared to other oxidizing agents due to its better stability, low cost, and easy to handle for the broad pH range [16,17]. Heptavalent manganese is the most powerful oxidant in all media (acidic, neutral, and alkaline) amongst various oxidation states of manganese [18–21]. The heptavalent manganese is also utilized as a disinfectant in water due to its ability to oxidize the organic matter [22,23]. Due to unpleasant color of heptavalent manganese, very low concentration of this promising oxidant is used for the removal of organic contaminants from the water to make it fit for drinking and to avoid the chromaticity in the water [24–26]. Hence, the use of catalyst becomes very essential for the removal of antiretroviral drug AZT with the minimum concentration of heptavalent manganese as oxidant.

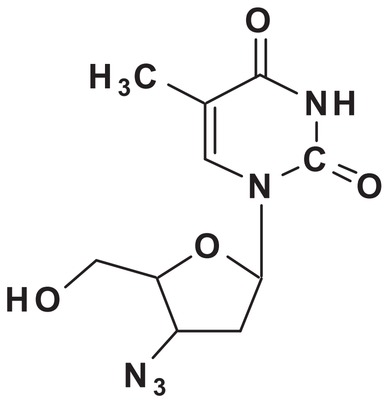

Fig. 1. Structure of Azidothymidine (AZT).

There are many transition metals which are used as catalyst to catalyze the redox reactions due to their variable oxidation states [27]. Ru^{3+} has an ability to catalyze many oxidative degradation transformations which includes the oxidation of ethers, alcohols, phenols, amines, and alkanes [28–30]. There are many investigations found in the literature on the use of aqueous Ru^{3+} for the catalytic oxidative degradation of D-panthenol, L-arginine, L-leucine, and L-isoleucine and atenolol in alkaline condition by heptavalent manganese [31–34]. Ru^{3+} homogeneous catalytic oxidations of Amitriptyline hydrochloride by permanganate, Thiamine by Chloramine T in acidic condition and levothyroxine by N-bromosuccinimide were reported in previous investigations [20,35,36]. There are no reports found in the literature on the studies of Ru^{3+}-catalyzed oxidative degradation of AZT by heptavalent manganese at environmentally relevant pH.

Therefore, the objective of the present investigation was to study the removal of AZT by Ru^{3+}-catalyzed oxidative degradation of AZT by heptavalent manganese at environmentally relevant pH. The effects of various parameters on the rate of the Ru^{3+} catalytic oxidative degradation reaction were studied thoroughly. The byproducts were identified and plausible catalytic mechanism is proposed on the basis of kinetic results.

2. Experiments and materials

2.1. Chemical reagents

The stock solutions of oxidant heptavalent manganese (MERCK Specialties Pvt Ltd) and antiretroviral drug AZT were prepared by dissolving a suitable amount of potassium permanganate and AZT in double-distilled water, respectively. After this the stock solution of heptavalent manganese was standardized using oxalic acid as per the laid down procedure in the literature [37]. The experiments of Ru^{3+}-catalyzed oxidative degradation of AZT by heptavalent manganese were performed at different pH using 0.02 mol dm^{-3} acetate, 0.02 mol dm^{-3} phosphate, and 0.02 mol dm^{-3} borate buffers for maintaining acidic, neutral, and basic conditions, respectively. The stock solution of the catalyst Ru^{3+} was prepared by mixing the required quantity of $RuCl_3$ (S. D. Fine Chem.) in suitable concentration of HCl for the catalytic degradation of AZT by heptavalent manganese. All experiments on the kinetics of the removal of AZT by heptavalent manganese in the presence of catalyst Ru^{3+} were performed using the freshly prepared solutions.

2.2. Instruments used for the kinetic studies and product analysis

A CARY 50 Bio UV–vis Spectrophotometer (Varian BV, the Netherlands) with temperature controller was used to measure absorbance of Ru^{3+} catalytic oxidative degradation of AZT by heptavalent manganese. High-performance liquid chromatography (HPLC) system (Shimadzu prominence) and high-resolution mass spectrophotometer (HR-MS) system (Thermo Scientific Q Exactive) along with a column Thermo Scientific Hypersil Gold C18 having dimension 150 × 4.6 mm–8 μm were used for the identification of the total eight products formed during the Ru^{3+} catalytic oxidative degradation of AZT by heptavalent manganese. Elico pH meter (Model Li 120) was used for the measurement of pH during the kinetic study of Ru^{3+} catalytic oxidative degradation of AZT by heptavalent manganese.

2.3. Kinetic procedure

The kinetics of Ru^{3+} catalytic oxidative degradation of AZT by heptavalent manganese was performed under pseudo-first-order conditions, where the concentration of AZT was maintained 10 times excess than the concentration of heptavalent manganese at constant temperature 25 ± 0.2˚C. All these solutions of analytical grade were kept in a thermostat to maintain uniform temperature. The catalytic oxidative degradation reaction was then initiated by mixing required quantities of thermostatted solutions. The progress of the catalytic oxidative degradation was observed spectrophotometrically by recording the absorbance (optical density) of non reacted heptavalent manganese at its wavelength $\lambda_{\max}$ 526 nm. The value of extinction coefficient was found $2{,}280 \pm 20\ \mathrm{dm^3\ mol^{-1}\ cm^{-1}}$ from the verification of Beer's law. This value of extinction coefficient is found to be close to the literature value of extinction coefficient [38]. During the Ru^{3+} catalytic oxidative degradation of AZT by heptavalent manganese, there was no significant interference from the other species [39]. The spectral changes oxidative degradation of AZT by heptavalent manganese were recorded using A CARY 50 Bio UV–vis Spectrophotometer at environmentally relevant pH and temperature 298 K [40]. The UV–visible spectral changes indicate that the concentration of heptavalent manganese decreases during the Ru^{3+} catalytic oxidative degradation of AZT by heptavalent manganese. The linear plots of log (absorbance) vs. time indicate that the order is unity with respect to oxidant heptavalent manganese at environmentally relevant pH.

2.4. Identification of the products formed during the catalytic oxidative degradation

The reaction mixture of pure AZT, excess concentration of heptavalent manganese over AZT, phosphate buffer, a very small concentration of catalyst Ru^{3+} were mixed and placed for the period of 24 h at the room temperature 25 ± 0.2˚C. After the period of 24 h, the reaction mixture was used for the analysis and identification of byproducts formed in this Ru^{3+}-catalyzed oxidative degradation of AZT by heptavalent manganese. High-performance liquid chromatography (HPLC) system (Shimadzu prominence) and HR-MS system (Thermo Scientific Q Exactive) were used for the analysis and identification of the byproducts formed in this catalytic degradation reaction. The HR-MS instrumental conditions for the analysis of the byproducts i.e. flow rate 500 μL/min, pressure 33.2 bar, mobile phase ratio 50:50 of acetonitrile, and water mixture were maintained carefully. A pump was used to offer a continuous flow of a solvent mixture of acetone and water (50:50) during the analysis. Then the reaction mixture traveled through a column C 18 and the different byproducts were separated based on their affinity. After this, the reaction mixture passed through a mass detector. Positive mode electrospray ionization (ESI^+) was used for the identification of the byproducts formed during the Ru^{3+}-catalyzed oxidative degradation of AZT by heptavalent manganese over the mass scan range 100–800 m/z. The total eight degraded products were identified from the HR-MS data. The mass spectrum of the pure antiretroviral drug AZT and eight byproducts formed during the Ru^{3+}-catalyzed oxidative degradation of AZT by heptavalent manganese at environmentally relevant pH are shown in Fig. 2 and listed in Table 1.

3. Results

3.1. Reaction orders

The oxidative degradation of antiretroviral drug AZT by heptavalent manganese takes place with a considerable rate at environmentally relevant pH. Experimental results indicate that orders with respect to AZT and heptavalent manganese are found to be unity. Therefore, the rate of the reaction for the uncatalyzed oxidative degradation of AZT by heptavalent manganese can be written as:

$$\text{Rate} = \frac{-\mathrm{d}[\mathrm{MnO_4^-}]}{\mathrm{d}t} = k_{\mathrm{U}}[\mathrm{Mn}^{7+}]^1[\mathrm{AZT}]^{0.75} \tag{1}$$

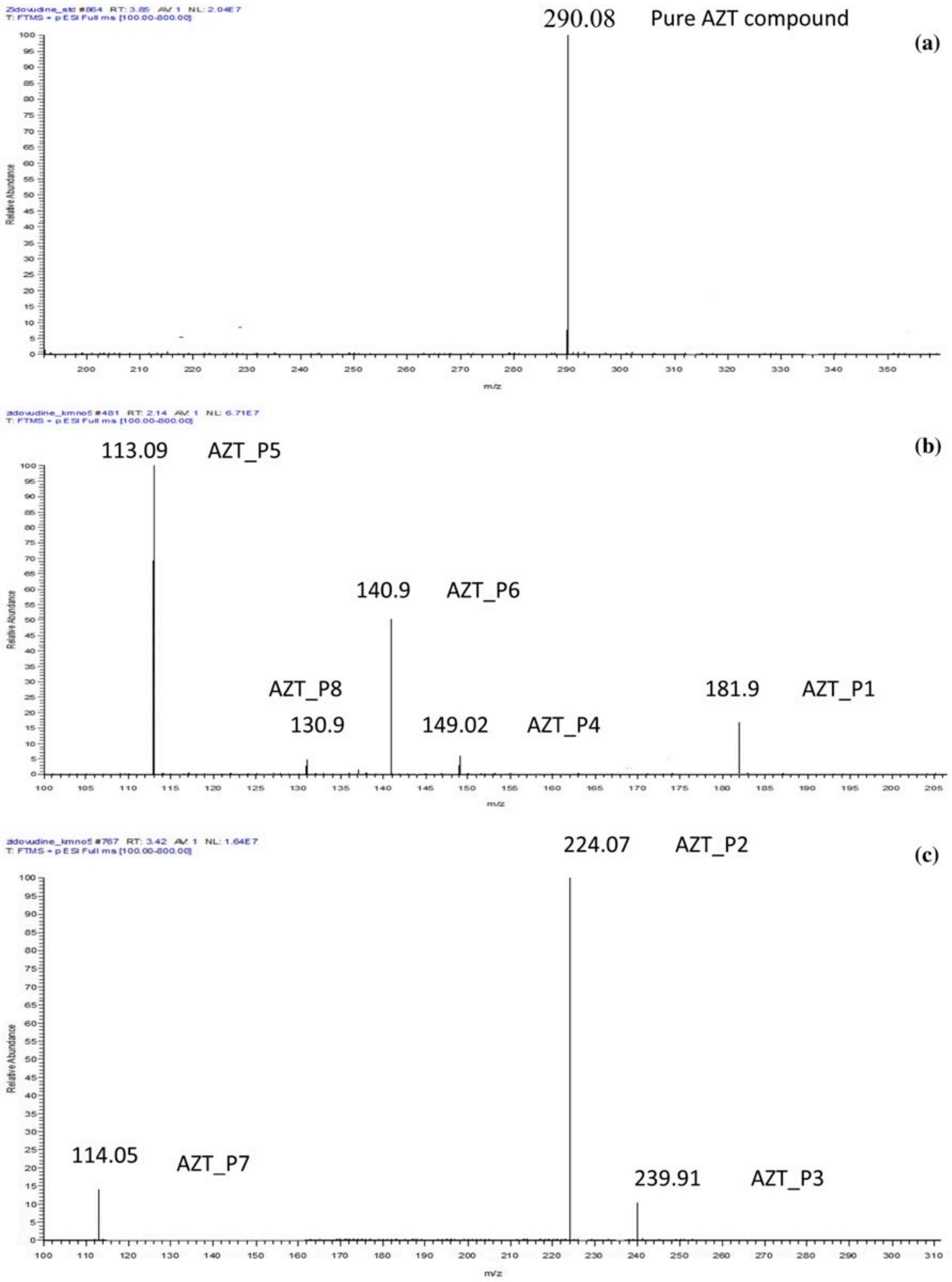

Fig. 2. HR-MS spectra of (a) pure AZT with its molecular ion peak m/z at 290.08, (b) oxidation products of Ru^{3+}-catalyzed AZT by heptavalent manganese at environmentally relevant pH with its molecular ion peaks m/z at 113.09 for AZT_P5, 130.9 for AZT_P8, 140.9 for AZT_P6, 149.02 for AZT_P4 and 181.9 for AZT_P1 and (c) oxidation product of Ru^{3+} AZT by heptavalent manganese at environmentally relevant pH with its molecular ion peaks m/z at 114.05 for AZT_P7, 224.07 for AZT_P2, 239.91 for AZT_P3.

Table 1
Identified degraded products of AZT during the Ru^{3+}-catalyzed oxidative degradation of AZT by heptavalent manganese at environmentally relevant pH and temperature 298 K by High-Resolution Mass Spectrometry (HR-MS) analysis

AZT Products	t_R $_{(Min)}$[a]	M + H^+/ M + Na^+ measured	Theoretical mass (Da)	Molecular formula	Difference in measured and theoretical mass	Name of the identified compounds
AZT_P1	2.14	181.96	181.10	$C_5H_6N_2O_4$	+0.86	3-Hydroxy-5-hydroxymethyl-1H-pyrimidine-2,4-dione
AZT_P2	3.42	224.07	224.21	$C_{10}H_{12}N_2O_4$	−0.14	1-(5-Hydroxymethyl-2,5-dihydro-furan-2-yl)-5-methyl-1H-pyrimidine-2,4-dione
AZT_P3	3.42	239.91	238.20	$C_{10}H_{10}N_2O_5$	+1.71	5-(5-Methyl-2,4-dioxo-3,4-dihydro-2H-pyrimidin-1-yl)-2,5-dihydro-furan-2-carboxylic acid
AZT_P4	3.42	149.02	126.11	$C_5H_6N_2O_2$	−0.08	5-Methyl-1H-pyrimidine-2,4-dione
AZT_P5	2.14	113.09	113.11	$C_5H_7NO_2$	−0.02	N-(2-Methyl-3-oxo-propenyl)-formamide
AZT_P6	2.14	140.90	141.13	$C_5H_7N_3O_2$	−0.23	(3-Azido-2,3-dihydro-furan-2-yl)-methanol
AZT_P7	2.14	114.05	115.13	$C_5H_9NO_2$	−1.08	(3-Amino-2,3-dihydro-furan-2-yl)-methanol
AZT_P8	2.14	130.90	131.13	$C_5H_9NO_3$	−0.23	(3-Hydroxyamino-2,3-dihydro-furan-2-yl)-methanol

[a] $t_{R(Min)}$ indicates retention time in minutes.

In this above Eq. (1), k_U is the rate constant for the uncatalyzed oxidative degradation of AZT by heptavalent manganese at environmentally relevant pH.

Ru^{3+}-catalyzed oxidative degradation of AZT by heptavalent manganese shows parallel paths with contributions from the uncatalyzed and catalyzed oxidative degradation of antiretroviral drug AZT by heptavalent manganese reactions (Eqs. (2)–(8)). Hence, the net reaction constant (k_N) using k_U (rate constant for the uncatalyzed reaction) and k_C (rate constant for the catalyzed reaction) can be expressed as:

$$k_N = k_U + k_C \tag{2}$$

The orders for the AZT, heptavalent manganese, and catalyst Ru^{3+} are determined from the slopes of log k_{obs} vs. log (concentration) by varying the concentrations of AZT, heptavalent manganese and catalyst Ru^{3+} while maintaining the others experimental conditions constant.

$$k_C = k_N - k_U \tag{3}$$

$$3Ru^{3+} + 4Mn^{7+} \longrightarrow 3Ru^{7+} + 4Mn^{4+} \tag{4}$$

$$Ru^{7+} + AZT \longrightarrow Ru^{3+} + AZT\ (\text{Oxidized}) \tag{5}$$

$$Ru^{3+} + Mn^{7+} \longrightarrow Ru^{6+} + Mn^{4+} \tag{6}$$

$$Ru^{6+} + AZT \longrightarrow Ru^{3+} + AZT\ (\text{Oxidized}) \tag{7}$$

$$Mn^{7+} + AZT \longrightarrow Mn^{4+} + AZT\ (\text{Oxidized}) \tag{8}$$

Using rate law, the rate of the Ru^{3+}-catalyzed oxidative degradation of AZT by heptavalent manganese reaction at environmentally relevant pH can be written as:

$$\text{Rate} = \frac{-d[MnO_4^-]}{dt} = k_N[Mn^{7+}][AZT] \tag{9}$$

$$\text{Rate} = \frac{-d[MnO_4^-]}{dt} = (k_U + k_C)[Mn^{7+}]^1[AZT]^1 \tag{10}$$

3.2. Influence of concentration of heptavalent manganese

The influence of variation in concentration of heptavalent manganese on uncatalyzed and Ru^{3+}-catalyzed oxidative degradation reactions of AZT by heptavalent manganese were investigated by varying the concentration of heptavalent manganese from 2.5×10^{-5} to 2.5×10^{-4} mol dm^{-3} while keeping other conditions fixed i.e. concentration of AZT = 1×10^{-3} mol dm^{-3}, concentration of Ru^{3+} = 3×10^{-7} mol dm^{-3}, concentration of buffer = 6×10^{-3} mol dm^{-3}, and Ionic strength (I) = 0.02 mol dm^{-3} in order to maintain pH and constant ionic strength at temperature 25 ± 0.2˚C. Plots of log (absorbance) vs. time for different concentration of permanganate were found in straight lines in both uncatalyzed and catalyzed oxidative degradation of AZT by heptavalent manganese. These plots show that the order with respect to heptavalent manganese is unity for both uncatalyzed and catalyzed oxidative degradation of AZT by heptavalent manganese at environmentally relevant pH.

3.3. Influence of concentration of AZT on the oxidative degradation reaction

The influence of variation in concentration of AZT on the uncatalyzed and Ru^{3+}-catalyzed oxidative degradation of AZT by heptavalent manganese reactions were investigated by varying the concentration of AZT from 5×10^{-4} to 3.0×10^{-3} mol dm^{-3} while keeping other reaction conditions constant i.e. concentration of heptavalent manganese = 1×10^{-4} mol dm^{-3}, concentration of Ru^{3+} = 3×10^{-7} mol dm^{-3}, concentration of buffer = 6×10^{-3} mol dm^{-3}, and Ionic strength (I) = 0.02 mol dm^{-3} in order to maintain pH and constant ionic strength at temperature 25 ± 0.2˚C. The kinetic outcome shows that the rate of the Ru^{3+} catalytic oxidative degradation of AZT by heptavalent manganese at environmentally relevant pH increases with the increase in the concentration of AZT. The plot of log k_{obs} vs. log [AZT] is plotted from the kinetic data. This plot found to be a straight line as shown in Fig. 3. The slope of the straight line plot shows the order with respect to AZT is unity (1.021).

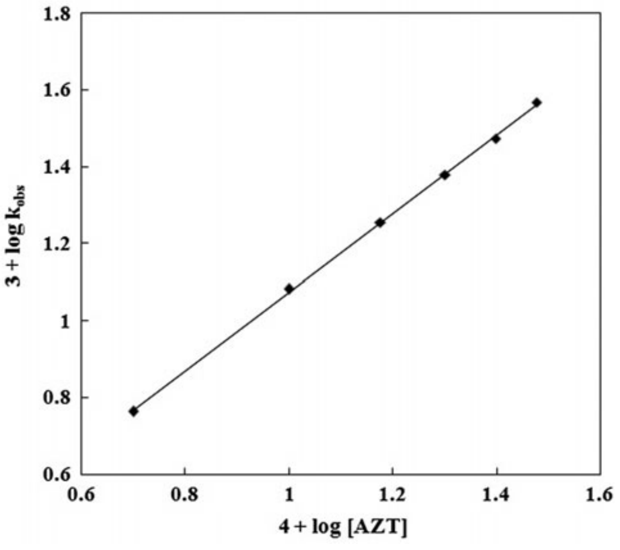

Fig. 3. Influence of variation in concentration of antiretroviral drug AZT on Ru^{3+}-catalyzed oxidative degradation of AZT by heptavalent manganese at environmentally relevant pH and temperature 298 K. [AZT] = 5×10^{-4} to 3×10^{-3} mol dm^{-3}, [Mn^{7+}] = 1×10^{-4} mol dm^{-3}, [Ru^{3+}] = 3×10^{-7} mol dm^{-3}, [Buffer] = 6×10^{-3} mol dm^{-3} and Ionic strength (I) = 0.02 mol dm^{-3}.

3.4. Influence of variation in ionic strength on the oxidative degradation reaction

In order to investigate the influence of variation in ionic strength on the uncatalyzed and Ru^{3+}-catalyzed oxidative degradation reaction of AZT by heptavalent manganese at environmentally relevant pH, the concentration of buffer was varied from 0.002 to 0.012 mol dm^{-3} while keeping other reaction conditions constant i.e. concentration of heptavalent manganese = 1×10^{-4} mol dm^{-3}, concentration of AZT = 1×10^{-3} mol dm^{-3}, and concentration of Ru^{3+} = 3×10^{-7} mol dm^{-3} at temperature 25 ± 0.2˚C. The kinetic results clearly indicate that there was no significant effect of variation in ionic strength on the uncatalyzed and catalyzed degradation reactions at environmentally relevant pH.

3.5. Influence of dielectric constant on the oxidative degradation reaction

The influence of variation in dielectric constant or solvent polarity was investigated by varying the concentration of the mixture of t-butanol and water while keeping other reaction conditions fixed i.e. concentration of heptavalent manganese = 1×10^{-4} mol dm^{-3}, concentration of AZT = 1×10^{-3} mol dm^{-3}, concentration of the Ru^{3+} = 3×10^{-7} mol dm^{-3}, concentration of buffer = 6×10^{-3} mol dm^{-3}, and Ionic strength (I) = 0.02 mol dm^{-3} in order to maintain pH and constant ionic strength at temperature 25 ± 0.2˚C for uncatalyzed and Ru^{3+}-catalyzed oxidative degradation of AZT by heptavalent manganese at environmentally relevant pH. The kinetic results of experiments show that as the volume of t-butanol increases or solvent polarity decreases, the rate of the uncatalyzed, and Ru^{3+}-catalyzed oxidative degradation of AZT by heptavalent manganese reactions decreases. Using experimental data, the graphs of log k_{obs} vs. $1/D$ was plotted for Ru^{3+}-catalyzed oxidative degradation of AZT by heptavalent manganese at environmentally relevant pH. This plot was found linear with negative slope as shown in Fig. 4. Similar results were reported in previous studies [20].

3.6. Influence of the initially added product MnO_2 on oxidative degradation reaction

The influence of the initially added product on the uncatalyzed and Ru^{3+}-catalyzed oxidative degradation of AZT by heptavalent manganese at environmentally relevant pH were investigated by adding MnO_2 in the reaction mixtures. The kinetic results indicate that there is a little catalytic effect of the addition of the MnO_2 on the uncatalyzed and Ru^{3+}-catalyzed oxidative degradation reactions at environmentally relevant pH because the increase in pH of the reaction mixture reduces the catalytic potential of the MnO_2 significantly [24].

3.7. Test for the involvement of free radical

In order to verify the involvement of formation of any free radical in uncatalyzed and Ru^{3+}-catalyzed oxidative degradation of AZT by heptavalent manganese at environmentally relevant pH, a required quantity of monomer acrylonitrile was added in both reaction mixtures separately and kept for 8 h in an inert atmosphere. These reaction mixtures were diluted using methanol. It was observed that there was no formation of any insoluble compound during the degradation reactions. This indicates that there is no involvement of any free radical in uncatalyzed and Ru^{3+}-catalyzed oxidative degradation of AZT reactions at environmentally relevant pH [41].

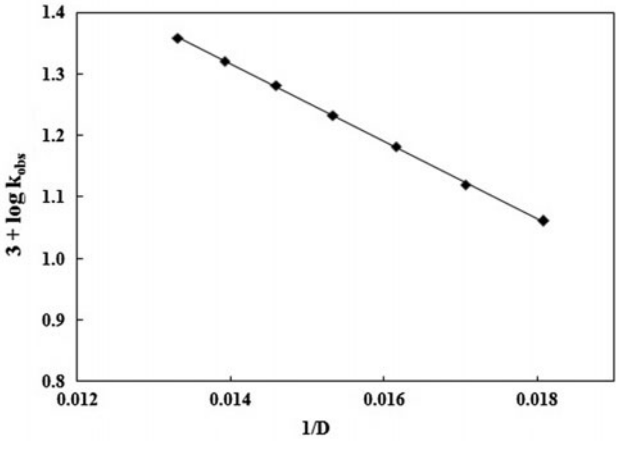

Fig. 4. Influence of variation in dielectric constant on Ru^{3+} oxidative degradation of AZT by heptavalent manganese at environmentally relevant pH and temperature 298 K by varying the concentration of t-butanol. $[Mn^{7+}] = 1 \times 10^{-4}$ mol dm^{-3}, $[AZT] = 1 \times 10^{-3}$ mol dm^{-3}, $[Ru^{3+}] = 3 \times 10^{-7}$ mol dm^{-3}, $[Buffer] = 6 \times 10^{-3}$ mol dm^{-3} and Ionic strength $(I) = 0.02$ mol dm^{-3}.

3.8. Influence of pH on the oxidative degradation reaction

The influence of variation in pH on the uncatalyzed and Ru^{3+}-catalyzed oxidative degradation of AZT by heptavalent manganese reactions were investigated at different pH from 3.0 to 9.0 while keeping other reaction conditions constant at temperature 25 ± 0.2℃. The kinetic results indicate that the rate constants of the uncatalyzed (k_U) and catalyzed (k_C) reactions are faster in acidic medium as compare to alkaline medium. The second-order rate constants for uncatalyzed (k''_U) and catalyzed (k''_C) reactions were evaluated by plotting the graph of k_{obs} vs. [AZT] at temperature 25 ± 0.2℃. Using these values of k''_U, k''_C and k''_N as given in Table 2, the graph of k''_{app} vs. pH is plotted as shown in Fig. 5. The influence of variation in pH has indicated that the apparent second-order rate constants are higher in acidic condition and lower in alkaline condition.

3.9. Influence of temperature on oxidative degradation reaction

The influence of variation in temperature on the uncatalyzed and Ru^{3+}-catalyzed oxidative degradation of AZT by heptavalent manganese reactions at environmentally relevant pH were investigated carefully at different temperatures 283, 288, 293, and 299 K by changing the concentration of AZT from 5×10^{-4} to 3.0×10^{-3} mol dm^{-3} and maintaining other reaction conditions constant i.e. concentration of heptavalent manganese = 1×10^{-4} mol dm^{-3}, concentration of catalyst $Ru^{3+} = 3 \times 10^{-7}$ mol dm^{-3}, concentration of buffer = 6×10^{-3} mol dm^{-3}, and Ionic strength (I) = 0.02 mol dm^{-3} in order to maintain pH and constant

Table 2
pH-dependent second-order-rate constants for the effect of variation in pH on the uncatalyzed and Ru^{3+}-catalyzed oxidative degradation of AZT by heptavalent manganese at different pH from 3.0 to 9.0 (temperature 298 K). $[Mn^{7+}] = 1 \times 10^{-4}$ mol dm^{-3}, $[AZT] = 1 \times 10^{-3}$ mol dm^{-3}, $[Ru^{3+}] = 3 \times 10^{-7}$ mol dm^{-3}, $[Buffer] = 6 \times 10^{-3}$ mol dm^{-3} and Ionic strength (I) = 0.02 mol dm^{-3}

pH	k''_U	k''_N	k''_C
3.0	6.35	56.80	50.45
4.0	5.32	48.15	42.83
5.0	4.13	40.96	34.55
6.0	3.59	33.06	28.72
7.0	2.69	25.37	21.55
8.0	1.65	19.08	13.43
9.0	1.18	11.36	7.16

Note: ±8% Error.

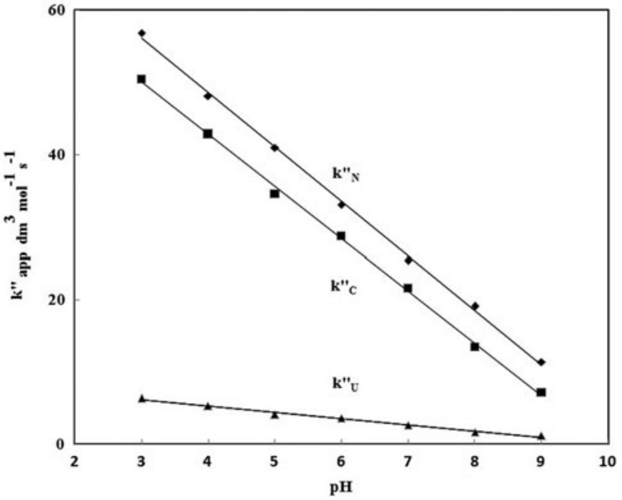

Fig. 5. pH-dependent second-order-rate constants for Ru^{3+} catalytic oxidative degradation of AZT by heptavalent manganese at different pH from 3.0 to 9.0 and temperature 298 K.

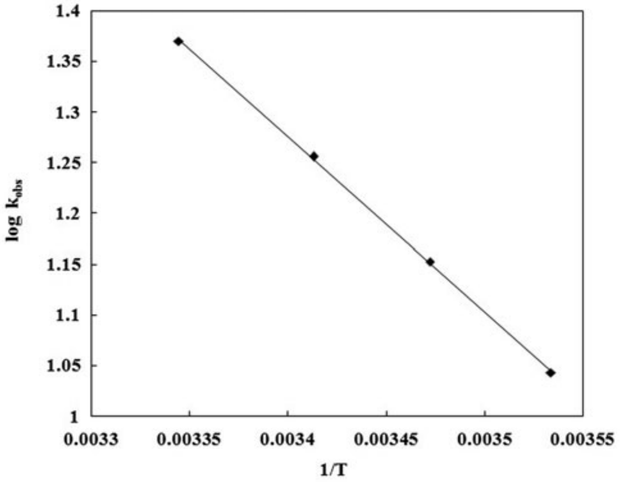

Fig. 6. Arrhenius plot log k vs. $1/T$ for four different temperatures 283, 288, 296 and 299 K by varying the concentration of AZT from 5×10^{-4} to 3×10^{-3} mol dm^{-3}, while freezing other experimental conditions such as $[MnO_4^-] = 1 \times 10^{-4}$ mol dm^{-3}, $[Ru^{3+}] = 3 \times 10^{-7}$ mol dm^{-3}, [Buffer] $= 6 \times 10^{-3}$ mol dm^{-3} and Ionic strength (I) = 0.02 mol dm^{-3}.

ionic strength. The kinetic results indicate that the rate constant values increase with increase in temperature from 283 to 299 K. From these rate constant values at different temperatures, the various activation parameters like E_a, $\Delta H^{\neq}$, $\Delta G^{\neq}$, and $\Delta S^{\neq}$ were determined using Arrhenius plots log k vs. $1/T$ for uncatalyzed and Ru^{3+}-catalyzed oxidative degradation of AZT by heptavalent manganese reactions at environmentally relevant pH as shown in Fig. 6.

3.10. *Influence of variation in concentration of catalyst Ru^{3+} on the rate of the reaction*

The influence of variation in concentration of Ru^{3+} catalyst on oxidative degradation of AZT by heptavalent manganese reaction at environmentally relevant pH was investigated carefully by varying concentration of Ru^{3+} from 1.0×10^{-7} to 1.0×10^{-6} mol dm^{-3} while keeping other reaction conditions fixed i.e. concentration of heptavalent manganese = 1×10^{-4} mol dm^{-3}, concentration of AZT = 1×10^{-3} mol dm^{-3}, concentration of Buffer = 6×10^{-3} mol dm^{-3}, and Ionic strength (I) = 0.02 mol dm^{-3} at temperature 25 ± 0.2°C. The kinetic data collected after performing an experiment shows that the rate of the reaction is faster in Ru^{3+}-catalyzed oxidative degradation of AZT by heptavalent manganese than uncatalyzed reaction. It clearly indicates that Ru^{3+} is an effective and potential catalyst for the removal of AZT by heptavalent manganese at environmentally relevant pH. The graph log k_{obs} vs. log $[Ru^{3+}]$ is plotted as shown in Fig. 7 using an experimental data. The nature of the graph is linear and order with respect to Ru^{3+} is found to be unity.

Activity of the Ru^{3+} catalyst:

It is observed by Moelwyn–Hughes [42] that the uncatalyzed and catalyzed reactions progress at the same time, for that the net reaction constant (k_N) can be written as:

$$k_N = k_U + K_C^* \, [Ru^{3+}]^n \tag{11}$$

here k_U is observed pseudo-first-order rate constant for uncatalyzed reaction while K_c^* is the catalytic constant for the Ru^{3+}-catalyzed reaction. The term "n" represents the order with respect to catalyst Ru^{3+}.

From the above Eq. (11), the value of the K_c^* can be calculated as follows:

$$K_C^* = \frac{[k_N - k_U]}{[Ru^{3+}]^n} = \frac{[k_C]}{[Ru^{3+}]^n} \quad \text{where } (k_N - k_U = k_C) \tag{12}$$

$$K_C^* = (4.69 \times 10^{-2})/(3 \times 10^{-7})$$

$$K_C^* = 1.56 \times 10^5$$

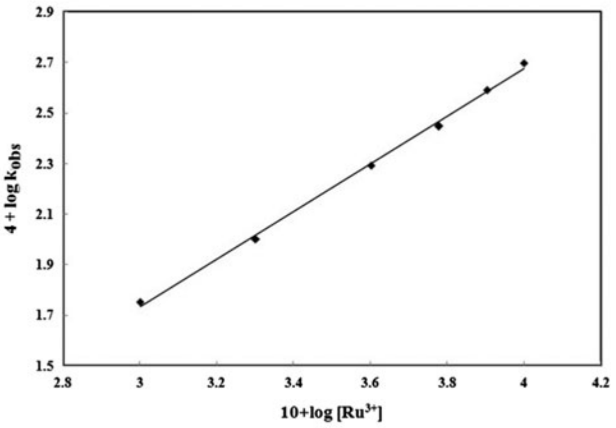

Fig. 7. Influence of variation in concentration of catalyst Ru^{3+} on oxidative degradation of AZT by heptavalent manganese at environmentally relevant pH (temperature 298 K). $[Ru^{3+}] = 1.0 \times 10^{-7}$ mol dm^{-3} to 1.0×10^{-6} mol dm^{-3}, $[Mn^{7+}] = 1 \times 10^{-4}$ mol dm^{-3}, $[AZT] = 1 \times 10^{-3}$ mol dm^{-3}, $[Buffer] = 6 \times 10^{-3}$ mol dm^{-3} and Ionic strength (I) = 0.02 mol dm^{-3}.

The above Eq. (12) can be rearranged as:

$$k_C = K_C^* \times [Ru^{3+}]^n \tag{13}$$

The above Eq. (13) after taking logarithm becomes:

$$\ln k_C = \ln K_C^* + n \ln [Ru^{3+}] \tag{14}$$

The straight line plot of the log K_C vs. log $[Ru^{3+}]$ shows the value of "n" i.e. order with respect to Ru^{3+} is unity. The intercept of the plot log K_C vs. log $[Ru^{3+}]$ gives the value of K_c^*. Using the above Eq. (13) and putting the values of orders with respect to catalyst Ru^{3+}, heptavalent manganese, and AZT, the Eq. (10) becomes:

$$\text{Rate} = \frac{-d[MnO_4^-]}{dt} = (k_U + K_C^*[Ru^{3+}]^1)[Mn^{7+}]^1[AZT]^1 \tag{15}$$

4. Discussion

The kinetic data for the catalyzed oxidative degradation of AZT by heptavalent manganese at environmentally relevant pH indicates that the orders are found to be unity with respect to heptavalent manganese, antiretroviral drug AZT, and catalyst Ru^{3+}. The effect of pH indicates that the rate of the removal of antiretroviral drug AZT reduces due to increase in the pH and decrease in the oxidation potential of heptavalent manganese. The values of apparent second-order rate constants (from pH 3.0 to 9.0) for the catalyzed reaction indicate that the rate of the removal of AZT increases at the higher concentration of H^+ and decreases at the lower concentration of H^+. At the higher concentration of H^+ or lower values of pH, the catalyst Ru^{3+} is oxidized to its higher oxidized forms Ru^{6+} and Ru^{7+} due to the higher oxidation potential of heptavalent manganese. During the oxidation of Ru^{3+} to higher oxidized forms by Mn^{7+}, Ru^{3+} reduces Mn^{7+} to Mn^{4+} which was also observed by the previous investigations [22,24,25]. Ru^{6+} and Ru^{7+} are having higher oxidation potential than the heptavalent manganese and hence they are better oxidizing agents than Mn^{7+}. Ru^{6+} is found to be unstable species due to its rapid conversion into hydroxide of ruthenium i.e. $Ru(OH)_4$. The antiretroviral drug AZT was degraded in a very small quantity by Ru^{6+} and gets reduced to the lower oxidized form Ru^{3+} during this redox reaction.

In order to investigate the catalytic effect of Ru^{3+}, Ru^{7+}, and Ru^{6+} separately, the kinetic experiments were performed using $KRuO_4$ (S. D. fine Chem.) and K_2RuO_4 (synthesized) according to the procedure reported by Greenwood and Earnshaw [43]. It was cleared from the kinetic data that Ru^{7+} is an efficient and potential cooxidant than Ru^{3+} and Ru^{6+}. The rate of removal of AZT at higher alkaline condition is very low due to the formation of a very small quantity of Ru^{6+} and Ru^{7+} for the Ru^{3+}-catalyzed oxidative degradation of AZT by heptavalent manganese. This is because of the very low oxidation potential of the heptavalent manganese at the higher alkaline pH.

A plausible catalytic mechanism (Scheme I) for the Ru^{3+}-catalyzed oxidative degradation of AZT by heptavalent manganese at environmentally relevant pH is proposed on the basis of kinetic data, chromatogram, and mass spectrum as shown in Fig. 8. In this mechanism, orders with respect to heptavalent manganese, Ru^{3+}, and AZT are taken unity.

The oxidative degraded products identified in uncatalyzed and Ru^{3+}-catalyzed oxidative degradation of AZT by heptavalent manganese were found same. There is interaction found between heptavalent manganese and Ru^{3+} in this catalytic mechanism. The eight products labeled as AZT_P1, AZT_P2, AZT_P3, AZT_P4, AZT_P5, AZT_P6, and AZT_P7 and AZT_P8 were identified during the catalytic oxidative degradation using mass spectrum. The structures of all these eight labeled degraded products formed after catalytic oxidative degradation of AZT by heptavalent manganese are shown in Fig. 9. AZT_P1 is formed due to the fragmentation of AZT and oxidation of methyl group to alcohol. Thymine compound AZT_P2

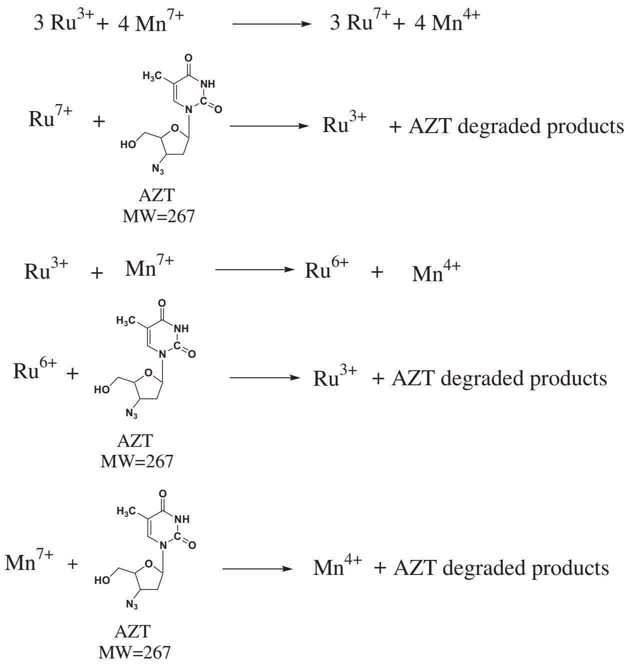

Fig. 8. The plausible catalytic mechanism of Ru^{3+}-catalyzed oxidative degradation of AZT by heptavalent manganese at environmentally relevant pH and temperature 298 K (Scheme I).

is formed due to the elimination of azide group from the ring. AZT_P3 is formed due to further oxidation of $–CH_2OH$ group of thymine to –COOH group. AZT_P4 is the fourth degraded product stavudine formed due to degradation of AZT. AZT_P5 is the fifth product formed containing two –CHO group due to breaking of ring of the stavudine. AZT_P6 is the next product formed after degradation of AZT. AZT_P7 is formed due to the removal of N_2 group from the product AZT_P6. AZT_P8 is the eighth product formed due to further oxidation of $–NH_2$ group to –NHOH group. In this Ru^{3+}-catalyzed mechanism, Ru^{7+} is the main active oxidized form of ruthenium which rapidly degrades AZT into different byproducts. Ru^{3+} is playing a catalytic role of electron shuttle for the elimination of AZT by its oxidative degradation at environmentally relevant pH and it is shown in Fig. 10. The catalytic role of the Ru^{3+} as electron shuttle was reported in the previous studies [22,24,25].

The reaction rates observed from the effect of variation in temperature indicates that the rate of removal of AZT is faster in the presence of Ru^{3+}-catalyzed reaction than uncatalyzed reaction.

$$\ln k = \ln A + \frac{E_a}{RT} \tag{16}$$

Using above Arrhenius Eq. (16) and Arrhenius plots of $\log k$ vs. $1/T$, the values of activation energy (E_a) in kJ mol^{-1} were calculated for the uncatalyzed and Ru^{3+}-catalyzed oxidative degradation of AZT by heptavalent manganese and is presented in Table 3. The smaller value of activation energy for Ru^{3+}-catalyzed reaction lowers the energy barrier of the Ru^{3+}-catalyzed oxidative degradation of AZT by heptavalent manganese than uncatalyzed reaction. It means that the lower value of E_a for Ru^{3+}-catalyzed reaction modifies the path of the oxidative degradation of AZT by heptavalent manganese at environmentally relevant pH. The other parameters i.e. activation enthalpy ($\Delta H^{\neq}$) and activation entropy ($\Delta S^{\neq}$) were determined from the Eyring equation [44]. The values of $\Delta H^{\neq}$ and $\Delta S^{\neq}$ are 42.90 k J mol^{-1} and $-135.40\ J\ mol^{-1}\ K^{-1}$, respectively, for uncatalyzed oxidative degradation of AZT by heptavalent manganese at environmentally relevant pH. Similarly, the values of $\Delta H^{\neq}$ and $\Delta S^{\neq}$ are 33.70 k J mol^{-1} and $-167.70\ J\ mol^{-1}\ K^{-1}$, respectively, for Ru^{3+}-catalyzed reaction. Using the values of $\Delta H^{\neq}$ and $\Delta S^{\neq}$, the values of activation Gibbs free energy $\Delta G^{\neq}$ were calculated. $\Delta G^{\neq}$ values for uncatalyzed and Ru^{3+}-catalyzed reactions are 82.30 and 79.40 kJ mol^{-1}, respectively. These values of $\Delta G^{\neq}$ show that the higher oxidized form of Ru^{3+} i.e. Ru^{7+} is a very reactive species and attacks on the antiretroviral drug AZT to form more ordered and tightly bound byproducts. $\Delta G^{\neq}$ and $\Delta H^{\neq}$ values are positive and indicate that the oxidative degraded byproducts of AZT are solvated. The calculated values of E_a, $\Delta G^{\neq}$, $\Delta S^{\neq}$ confirms that the homogeneous catalyst Ru^{3+} oxidizes quickly to the higher oxidize form Ru^{7+} by heptavalent manganese as compare to other catalyst. This higher oxidized form Ru^{7+} degrades rapidly antiretroviral drug AZT and increases the higher reducing property of AZT as compare to uncatalyzed reaction. The projected Ru^{3+}-catalyzed mechanism for the oxidative degradation of AZT by heptavalent manganese at environmentally relevant pH is in good agreement with rate law.

The effect of variation in ionic strength on the uncatalyzed and Ru^{3+}-catalyzed oxidative degradation reactions show that the effect of variation in ionic strength is negligible on both these reactions. This confirms that oxidative degradation reaction is between neutral and charged species or two neutral species [45]. The effect of variation in dielectric constant by varying the concentration of tertiary butanol on the uncatalyzed and Ru^{3+}-catalyzed oxidative degradation of AZT by heptavalent manganese reactions at environmentally relevant pH indicates that the reaction is between two dipoles [46].

AZT_P1

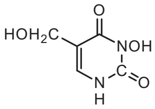

3-Hydroxy-5-hydroxymethyl-1*H*-pyrimidine-2,4-dione

AZT_P2

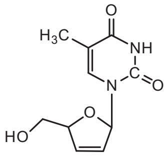

1-(5-Hydroxymethyl-2,5-dihydro-furan-2-yl)-5-methyl-1*H*-pyrimidine-2,4-dione

AZT_P3

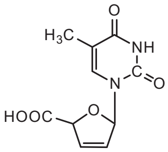

5-(5-Methyl-2,4-dioxo-3,4-dihydro-2*H*-pyrimidin-1-yl)-2,5-dihydro-furan-2-carboxylic acid

AZT_P4

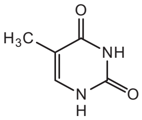

5-Methyl-1*H*-pyrimidine-2,4-dione

AZT_P5

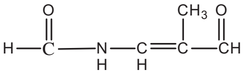

$$H{-}C(=O){-}NH{-}CH{=}C(CH_3){-}CHO$$

N-(2-Methyl-3-oxo-propenyl)-formamide

AZT_P6

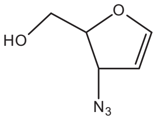

(3-Azido-2,3-dihydro-furan-2-yl)-methanol

AZT_P7

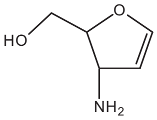

(3-Amino-2,3-dihydro-furan-2-yl)-methanol

AZT_P8

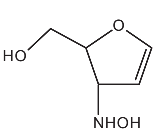

(3-Hydroxyamino-2,3-dihydro-furan-2-yl)-methanol

Fig. 9. Eight degraded products formed during the Ru^{3+}-catalyzed oxidative degradation of AZT by heptavalent manganese at environmentally relevant pH and termperature 298 K.

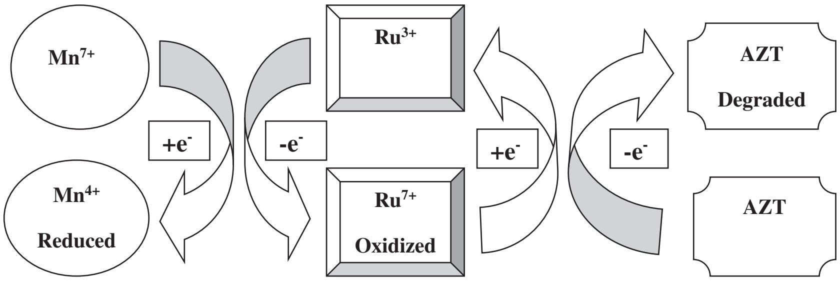

Fig. 10. The catalytic role of catalyst Ru^{3+} as electron shuttle in oxidative degradation of AZT by heptavalent manganese at environmentally relevant pH and temperature 298 K.

Table 3
Activation parameters from the influence of variation in temperature for uncatalyzed and Ru^{3+}-catalyzed oxidative degradation of AZT by heptavalent manganese at environmentally relevant pH. [Mn^{7+}] = 1 × 10^{-4} mol dm^{-3}, [AZT] = 5 × 10^{-4} to 3 × 10^{-3} mol dm^{-3}, [Ru^{3+}] = 3 × 10^{-7} mol dm^{-3}, [Buffer] = 6 × 10^{-3} mol dm^{-3} and Ionic strength (I) = 0.02 mol dm^{-3}

Activation parameters	Values uncatalyzed	Values Ru^{3+}-catalyzed
E_a (kJ mol^{-1})	45.30 ± 2.00	33.10 ± 2.00
$\Delta H^{\neq}$ (kJ mol^{-1})	42.90 ± 2.00	33.70 ± 1.50
$\Delta S^{\neq}$ (Jk^{-1} mol^{-1})	−135.40 ± 14.20	−167.70 ± 13.20
$\Delta G^{\neq}$ (kJ mol^{-1})	82.30 ± 7.40	79.40 ± 6.30

5. Conclusion

Mechanistic and spectroscopic investigations of Ru^{3+}-catalyzed oxidative degradation of AZT by heptavalent manganese at environmentally relevant pH were investigated for the first time. The rate of the Ru^{3+}-catalyzed oxidative degradation of AZT by heptavalent manganese at environmentally relevant pH is found eight times faster than uncatalyzed reaction. The effect of pH concludes that the medium plays a very crucial role in this catalytic oxidative degradation reaction. The rate of the removal of the AZT by heptavalent manganese in the presence of catalyst Ru^{3+} at temperature 25 ± 0.2°C is faster in strongly acidic medium than in strongly alkaline medium due to decrease in the oxidation potential of heptavalent manganese from acidic to alkaline conditions. The total number of eight products are analyzed and identified in the Ru^{3+}-catalyzed and uncatalyzed oxidative degradation reactions. The degraded products formed in both uncatalyzed and Ru^{3+}-catalyzed reactions are found same. The kinetic outcome concludes that the orders are found unity for the heptavalent manganese, catalyst Ru^{3+}, and the antiretroviral drug AZT. The smaller value of activation energy E_a for the Ru^{3+}-catalyzed reaction than uncatalyzed reaction concludes that Ru^{3+} is a potential and versatile catalyst for the removal of AZT by heptavalent manganese at environmentally relevant pH. The negative value of the $\Delta S^{\neq}$ shows that the higher oxidized form Ru^{7+} attacks on the antiretroviral drug AZT to form more ordered byproducts. The projected catalytic mechanism for Ru^{3+}-catalyzed oxidative degradation of AZT by heptavalent manganese at environmentally relevant pH is in agreement with the experimental results. This projected Ru^{3+} catalytic mechanism shows that the higher oxidized form of ruthenium i.e. Ru^{7+} is very active species and catalyzes the oxidative degradation of the antiretroviral drug AZT by heptavalent manganese effectively at environmentally relevant pH. Ru^{3+} acts as an electron shuttle which reduces heptavalent manganese to Mn^{4+}. This investigation clearly concludes that the catalyst Ru^{3+} is a very efficient and potential catalyst for the removal of antiretroviral drug AZT by heptavalent manganese at environmentally relevant pH.

References

[1] World Health Organization, Pharmaceuticals in Drinking-water, Geneva, 2011.

[2] B. Lubliner, M. Redding, S. Golding, D. Ragsdale, Pharmaceuticals and Personal Care Products in Wastewater Treatment Systems, Department of Ecology, Environmental Assessment Program, Washington, DC, 2008.

[3] T. Heberer, Occurrence, fate, and removal of pharmaceutical residues in the aquatic environment: A review of recent research data, Toxicol. Lett. 131 (2002) 5–17.

[4] D.J. Lapworth, N. Baran, M.E. Stuart, R.S. Ward, Emerging organic contaminants in groundwater: A review of sources, fate and occurrence, Environ. Pollut. 163 (2012) 287–303.

[5] H. Yuan, X. Zhou, Y.L. Zhang, Degradation of acid pharmaceuticals in the UV/H_2O_2 process: Effects of humic acid and inorganic salts, CLEAN—Soil Air Water 41 (2013) 43–50.

[6] R.M. Kulkarni, M.S. Hanagadakar, R.S. Malladi, M.S. Gudaganatti, H.S. Biswal, S.T. Nandibewoor, Transformation of linezolid during water treatment with chlorine: A kinetic study, Indian J. Chem. Technol. 21 (2014) 38–43.

[7] M.S. Gudaganatti, M.S. Hanagadakar, R.M. Kulkarni, R.S. Malladi, R.K. Nagarale, Transformation of levofloxacin during water chlorination process: Kinetics and pathways, Prog. React. Kinet. Mech. 37 (2012) 366–382.

[8] I.R. Bautitz, R.F.P. Nogueira, Degradation of tetracycline by photo-Fenton process—Solar irradiation and matrix effects, J. Photochem. Photobiol., A 187 (2007) 33–39.

[9] R.F.P. Nogueira, J.R. Guimaraes, Photodegradation of dichloro acetic acid and 2, 4-dichlorophenol by ferrioxalate /H_2O_2 System, Water Res. 34 (2000) 895–901.

[10] P. Kumar, P.S. Keshava Kumar, R.M. Kulkarni, Fate of zidovudine through water treatment with chlorine: A kinetic study, Int. Res. J. Environ. Sci. 3 (2014) 50–55.

[11] M.A. Fischl, D.D. Richman, M.H. Grieco, M.S. Gottlieb, P.A. Volberding, O.L. Laskin, J.E. Leedom, J.E. Groopman, D. Mildvan, D. Mildran, R.T. Schooley, The efficacy of azidothymidine (AZT) in the treatment of patients with AIDS and AIDS related complex. A double-blind placebo control trial, N. Engl. J. Med. 317 (1987) 185–191.

[12] A.R. Gennaro, Remington: The Science and Practice of Pharmacy, nineteenth ed., vol. II, Mack Publishing, Easton, PA, 1995, pp. 1332–1336.

[13] S. Budavari, The Merck Index, twelfth ed., Merck & Co., White House Station, NJ, 1996, pp. 732–740.

[14] E. Rodríguez, A. Sordo, J.S. Metcalf, J.L. Acero, Kinetics of the oxidation of cylindrospermopsin and anatoxin-a with chlorine, monochloramine and permanganate, Water Res. 41 (2007) 2048–2056.

[15] E. Rodríguez, M.E. Majado, J. Meriluoto, J.L. Acero, Oxidation of microcystins by permanganate: Reaction kinetics and implications for water treatment, Water Res. 41 (2007) 102–110.

[16] R.H. Waldemer, P.G. Tratnyek, Kinetics of contaminant degradation by permanganate, Environ. Sci. Technol. 40 (2006) 1055–1061.

[17] X.H. Guan, D. He, J. Ma, G.H. Chen, Application of permanganate in the oxidation of micro pollutants: A mini review, Front. Environ. Sci. Eng. China 4 (2010) 405–413.

[18] R.M. Kulkarni, D.C. Bilehal, S.T. Nandibewoor, Deamination and decarboxylation in the chromium(III)-catalyzed oxidation of L-valine by alkaline permanganate and analysis of chromium(III) in microscopic amounts by a kinetic method, Transition Met. Chem. 28 (2003) 199–208.

[19] D.C. Bilehal, R.M. Kulkarni, S.T. Nandibewoor, Comparative study of the chromium(III) catalysed oxidation of l-leucine and l-isoleucine by alkaline permanganate: A kinetic and mechanistic approach, J. Mol. Catal. A: Chem. 232 (2005) 21–28.

[20] J.C. Abbar, S.D. Lamani, S.T. Nandibewoor, Ruthenium(III) catalyzed oxidative degradation of amitriptyline-A tricyclic antidepressant drug by permanganate in aqueous acidic medium, J. Sol. Chem. 40 (2011) 502–520.

[21] A.A.P. Khan, A. Mohd, S. Bano, A. Husain, K.S. Siddiqi, Kinetic and mechanistic investigation of the oxidation of the antibacterial agent levofloxacin by permanganate in alkaline medium, Transition Met. Chem. 35 (2010) 117–123.

[22] J. Zhang, X. Guan, Ru(III)-catalyzed permanganate oxidation of bisphenol A, Desalin. Water Treat. 52 (2014) 4592–4601.

[23] T. Lin, S. Pan, W. Chen, C. Yu, Effect of potassium permanganate pre-oxidation on fouling and pore size of ultrafiltration membrane for drinking water treatment, Desalin. Water Treat. 50 (2012) 254–263.

[24] J. Zhang, Y. Zhang, H. Wang, X. Guan, Ru(III) catalyzed permanganate oxidation of aniline at environmentally relevant pH, J. Environ. Sci. 26 (2014) 1395–1402.

[25] J. Zhang, B. Sun, H.X. Guan, H. Wang, L.H. Bao, Y.Y. Huang, Ruthenium nano particles supported on CeO_2 for catalytic permanganate oxidation of butylparaben, Environ. Sci. Technol. 47 (2013) 13011–13019.

[26] J. Zhang, B. Sun, X. Xiong, N. Gao, W. Song, E. Du, X. Guan, G. Zhou, Removal of emerging pollutants by Ru/TiO_2-catalyzed permanganate oxidation, Water Res. 63 (2014) 262–270.

[27] A.K. Das, Kinetic and mechanistic aspects of metal ion catalysis in cerium(IV) oxidation, Coord. Chem. Rev. 213 (2001) 307–325.

[28] A.K. Singh, A.K. Singh, V. Singh, S. Rahmani, A. Singh, B. Singh, Ru(III) catalysed oxidation of diethanolamine and triethanolamine by Br(V) in presence of perchloric acid, J. Chem. Res. 2006 (2006) 56–63.

[29] B. Singh, A.K. Singh, K.L. Singh, R. Dubey, S.K. Singh, Mechanism of Ru(III) catalysis in potassium bromate oxidation of dimethyl sulphoxide in perchloric acid. A kinetic approach, Oxid. Commun. 34 (2011) 526–532.

[30] A. Saha, B.C. Ranu, Ruthenium(III)-catalysed phenylselenylation of allyl acetates by diphenyl diselenide and indium(I) bromide in neat: Isolation and identification of intermediate, Org. Biomol. Chem. 9 (2011) 1763–1767.

[31] R.V. Hosahalli, A.P. Savanur, S.T. Nandibewoor, S.A. Chimatadar, Kinetics and mechanism of uncatalysed and ruthenium(III)-catalysed oxidation of d-panthenol by alkaline permanganate, Transition Met. Chem. 35 (2010) 237–246.

[32] N.N. Halligudi, S.M. Desai, S.T. Nandibewoor, Free radical intervention, deamination and decarboxylation in the ruthenium(III)-catalyzed oxidation of L-arginine by alkaline permanganate-A kinetic study, Transition Met. Chem. 26 (2001) 28–35.

[33] A.K. Kini, S.A. Farokhi, S.T. Nandibewoor, A comparative study of ruthenium(III) catalyzed oxidation of L-leucine and L-isoleucine by alkaline permanganate: A kinetic and mechanistic approach, Transition Met. Chem. 27 (2002) 532–540.

[34] R.M. Mulla, G.C. Hiremath, S.T. Nandibewoor, Kinetic, mechanistic and spectral investigation of ruthenium(III)-catalysed oxidation of atenolol by alkaline permanganate (stopped-flow technique), J. Chem. Sci. 117 (2005) 33–42.

[35] A.A.P. Khan, A. Khan, A.M. Asiri, A.K. Singh, Homogenous catalysis of Ru(III) for the oxidation of thiamine by chloramine T in acidic medium, Int. J. Electrochem. Sci. 10 (2015) 759–774.

[36] A.A.P. Khan, A. Khan, A.M. Asiri, N. Azum, M.A. Rub, Micro concentrations of Ru(III) used as homogenous catalyst in the oxidation of levothyroxine by N-bromosuccinimide and the mechanistic pathway, J. Taiwan Inst. Chem. Eng. 45 (2014) 127–133.

[37] G.H. Jeffery, J. Bassett, J. Mendham, R.C. Denney, Vogel's Textbook of Quantitative Chemical Analysis, fifth ed., ELBS, Longman, Essex, 1996, p. 370.

[38] G.C. Hiremath, R.M. Kulkarni, S.T. Nandibewoor, Kinetics of oxidative degradation and deamination of atenolol by aqueous alkaline permanganate, Indian J. Chem. 44 (2005) 245–250.

[39] L.I. Simandi, M. Jaky, C.R. Savage, Z.A. Schelly, Kinetics and mechanism of the permanganate ion oxidation of sulfite in alkaline solutions. The nature of short—Lived intermediates, J. Am. Chem. Soc. 107 (1985) 4220–4224.

[40] R.M. Kulkarni, V.S. Bhamare, B. Santhakumari, Oxidative transformation of antiretroviral drug zidovudine during water treatment with permanganate: Reaction kinetics and pathways, Desalin. Water Treat. (2016), doi: 10.1080/19443994.2016.1149110.

[41] S. Bhattacharya, P. Banerjee, Kinetic studies on the electron transfer between azide and nickel(IV) oxime imine complexes in aqueous Solution, Bull. Chem. Soc. Jpn. 69 (1996) 3475–3482.

[42] E.A. Moelwyn-Hughes, Kinetics of Reaction in Solutions, Oxford University Press, London, 1947.

[43] N.N. Greenwood, A. Earnshaw, Chemistry of Elements, Pergamon Press, Oxford, 1997.

[44] A.A.P. Khan, A.M. Asiri, N. Azum, M.A. Rub, A. Khan, A.O. Al-Youbi, Kinetics and mechanistic investigation of decarboxylation for the oxidation of levofloxacin by chloramine-T in acidic medium, Ind. Eng. Chem. Res. 51 (2012) 4819–4824.

[45] K.J. Laidler, Chemical Kinetics, third ed., vol. 183, Pearson Education, Singapore, Indian Branch, Delhi, India, 2004, pp. 198–199.

[46] E.S. Amis, Solvent Effects on Reaction Rates and Mechanisms, Academic Press, New York, NY, 1966.